Journal of Gastroenterology and Hepatology

WILEY | JGHF Journal of Gastroenterology and Hepatology Foundation

ORIGINAL ARTICLE - HEPATOLOGY (CLINICAL) OPEN ACCESS

Diagnostic Value of MR Elastography and MRI-Proton Density Fat Fraction in Cirrhosis Based on Explant Liver Histology

Eun-Ki Min[1] | Seung-seob Kim[2] | Byungsoo Ahn[3] | Deok-Gie Kim[1] | Dong Jin Joo[1] | Sang Hoon Ahn[4] | Seung Up Kim[4] | Jae Geun Lee[1]

[1]Department of Surgery, The Research Institute for Transplantation, Yonsei University College of Medicine, Seoul, Republic of Korea | [2]Department of Radiology and Research Institute of Radiological Science, Yonsei University College of Medicine, Seoul, Republic of Korea | [3]Department of Pathology, Yonsei University College of Medicine, Seoul, Republic of Korea | [4]Department of Internal Medicine, Yonsei University College of Medicine, Seoul, Republic of Korea

Correspondence: Seung Up Kim (ksukorea@yuhs.ac) | Jae Geun Lee (drjg1@yuhs.ac)

Received: 9 September 2025 | **Revised:** 26 January 2026 | **Accepted:** 17 February 2026

Keywords: advanced fibrosis | cirrhosis | liver transplantation | magnetic resonance elastography | proton density fat fraction

ABSTRACT

Background and Aims: Accurate assessment of advanced fibrosis and steatosis is essential for prognostication in chronic liver disease. This study aimed to evaluate the diagnostic performance of MRI in assessing liver fibrosis and steatosis in patients undergoing liver transplantation (LT).

Methods: Patients who underwent LT between January 2019 and December 2023 with pretransplant MR elastography (MRE) and MRI-based proton density fat fraction (MRI-PDFF) examinations were included. Explanted livers were assessed for fibrosis and steatosis, with cirrhosis subclassified using the Laennec system. Diagnostic performance was evaluated using area under the receiver operating characteristic curve (AUC) analysis.

Results: Among 187 patients (median age, 57 years), 72.2% were male. Hepatitis B virus (55%) and alcoholic liver disease (21.4%) were the most common etiologies. The median Model for End-Stage Liver Disease (MELD) score was 11. MRE detected cirrhosis (F4) with an AUC of 0.92 (95% confidence interval [CI], 0.87–0.97) and severe cirrhosis (F4c) with an AUC of 0.85 (95% CI, 0.79–0.91), at threshold values of 4.76 and 6.43 kPa, respectively. MRI-PDFF identified steatosis with an AUC of 0.83 (95% CI, 0.76–0.89) at a threshold of 2.80%. Comparisons of patients stratified by the threshold values for cirrhosis and severe cirrhosis revealed significant differences in MELD scores, history of portal hypertension-related complications, liver function parameters, and intraoperative transfusion requirements (all $p < 0.05$).

Conclusions: MRI demonstrated high diagnostic accuracy for detecting cirrhosis and steatosis in patients with advanced fibrosis undergoing LT. MRE further stratified cirrhosis severity, suggesting clinical applicability in cirrhosis staging and risk assessment.

Abbreviations: AST, aspartate aminotransferase; AUC, area under the receiver operator characteristic curve; BMI, body mass index; CHB, chronic hepatitis B; CI, confidence interval; CLD, chronic liver disease; CTP, Child–Pugh; HCC, hepatocellular carcinoma; HR, hazard ratio; INR, international normalized ratio; IQR, interquartile range; LT, liver transplantation; MASLD, metabolic dysfunction-associated steatotic liver disease; MELD, model for end-stage liver disease; MRE, magnetic resonance elastography; MRI-PDFF, MRI proton density fat fraction; RBC, red blood cell; ROI, region of interest.

Eun-Ki Min and Seung-seob Kim contributed equally to this work.

1 | Introduction

Accurate assessment and early detection of advanced liver fibrosis are critical for guiding medical intervention, monitoring treatment response, and identifying patients with chronic liver disease (CLD) who are at high risk of hepatic decompensation and hepatocellular carcinoma (HCC) [1–3]. Precise evaluation of hepatic steatosis is also essential for treatment planning in patients with metabolic dysfunction-associated steatotic liver disease (MASLD) [4].

While histologic evaluation remains the gold standard for fibrosis staging and steatosis grading, its invasiveness and bleeding risk limit its use, particularly in patients with coagulopathy [5]. To address this, various noninvasive tests have been developed [6]. Among these, MR elastography (MRE) has demonstrated the highest diagnostic accuracy for fibrosis staging [7–9], and MRI-based proton density fat fraction (MRI-PDFF) has shown high performance in quantifying hepatic steatosis [10, 11].

Despite their utility, the diagnostic performance of MRE and MRI-PDFF has not been thoroughly evaluated in patients with advanced fibrosis, especially those with cirrhosis, because of challenges in liver biopsy in this population [12]. Cirrhosis represents a heterogeneous spectrum with varying degrees of fibrotic burden and clinical manifestations, ranging from compensated to decompensated stages, requiring refined assessment for accurate prognostication. In addition to clinical staging systems, such as the Child–Pugh (CTP) score, the severity of cirrhosis can be histologically subclassified based on fibrous septal thickness and nodule size, as described in the Laennec system, which is a refinement of the METAVIR scoring system [13]. This histologic subclassification has been shown to correlate with portal hypertension, hepatic decompensation, and liver-related mortality [13–16].

Most patients undergoing liver transplantation (LT) present with advanced fibrosis, predominantly cirrhosis. Explanted livers at LT provide a unique opportunity for comprehensive histologic assessment of both fibrosis and steatosis, enabling robust validation of MRI-based diagnostic modalities in this population.

This study aimed to evaluate the diagnostic accuracy of pretransplant MRE and MRI-PDFF in patients undergoing LT and whether MRE-based liver stiffness can stratify the histologic and clinical stages of cirrhosis.

2 | Materials and Methods

This research adhered to the principles outlined in the Declaration of Helsinki and the Declaration of Istanbul and was approved by the Institutional Review Board at Severance Hospital, part of the Yonsei University Health System (IRB No. 4–2024-0284). The requirement for informed consent was waived owing to the retrospective nature of the study.

2.1 | Study Population

Between January 2019 and December 2023, 704 patients underwent LT at our center. Of these, 190 patients underwent liver MRI examination, including MRE and MRI-PDFF, within 3 months prior to surgery. At our center, MRE/MRI-PDFF is performed as part of follow-up imaging for patients on the liver transplant waiting list. Patients who declined MRI evaluation due to insurance coverage issues did not undergo MRE/MRI-PDFF, and those undergoing deceased donor LT or emergent living donor LT often did not undergo MRI evaluation due to insufficient time. Among the 190 patients, there were no cases of retransplantation or pediatric LT. After excluding patients undergoing combined solid organ transplantation ($n = 3$), a total of 187 patients were included in the study.

2.2 | Data Collection and Definitions

Collected data included etiology of liver disease, CTP score, degrees of ascites, esophageal varices, encephalopathy, pretransplant model for end-stage liver disease (MELD) score, donor characteristics, ABO incompatibility, and operation-related data. Laboratory parameters, including platelet count, serum bilirubin, alkaline phosphatase, aspartate aminotransferase (AST), alanine aminotransferase, albumin, fasting glucose, gamma-glutamyl transferase, alpha-fetoprotein, des-gamma carboxyprothrombin, prothrombin time (international normalized ratio [INR]), and C-reactive protein, were collected at the time of LT.

The graft-to-recipient weight ratio was calculated as (graft weight [g] /recipient weight [kg]) × 100. Graft loss was defined as the need for retransplantation or patient death. Graft survival was monitored for up to 1 year after LT, with the final follow-up in December 2024.

2.3 | MRI-Based Assessment of Liver Stiffness and Steatosis

MRE and MRI-PDFF were performed using the 3.0-T scanner (Discovery 750w, GE Healthcare, Milwaukee, WI, USA). The median interval between MRI and LT was 6 days. One radiologist with more than 10 years of experience in abdominal radiology measured liver stiffness and steatosis.

For liver stiffness measurement on MRE, up to four free-hand regions of interest (ROIs) were drawn on the magnitude image. Areas covered by the 95% confidence grid, within 1 cm of the liver capsule, the gallbladder fossa, around major intrahepatic vessels, and "hot spots" were avoided. "Hot spots" refer to focal areas of increased stiffness relative to the surrounding liver, often found near the liver dome or directly beneath the passive driver. These ROIs were then transferred to the grayscale elastogram image by copy/pasting. The final liver stiffness was calculated using the weighted arithmetic mean: $(m_1w_1 + m_2w_2 + m_3w_3 + m_4w_4) \div (w_1 + w_2 + w_3 + w_4)$, where m_1–m_4 represent the average liver stiffness values of each sampled area and w_1–w_4 correspond to the respective ROI sizes [5, 17].

To measure steatosis using PDFF, the mean values of the four ROIs were calculated. Each ROI measured $\geq 4\,cm^2$ and was placed in the right anterior, right posterior, left medial, and left lateral segments, avoiding large intrahepatic vessels [18].

2.4 | Histopathologic Assessment of Explanted Liver

Seven nontumor areas were evenly sampled from the explanted liver to ensure representative coverage, including three samples from each of the right and the left lobes and one additional sample for broader representation. The samples were embedded in paraffin, sectioned at 4 μm, and stained with hematoxylin and eosin. One slide was additionally stained with Masson's trichrome to assess fibrosis. An experienced pathologist, blinded to the patient's radiologic data, assessed the processed slides.

The degree of fibrosis was evaluated according to the Laennec system, as previously described [14]. Inflammatory activity was scored separately for the lobular and septal area as follows: A0 (none), A1 (mild), A2 (moderate), and A3 (severe). The final inflammatory activity score was determined based on the higher grade observed between the lobular and septal regions. Steatosis was graded based on the percentage of fat-containing hepatocytes: S0 (< 5%), S1 (5%–33%), S2 (34%–66%), and S3 (> 66%). To best reflect the overall disease burden, the highest grade observed among the seven slides was recorded as the final assessment.

2.5 | Statistical Analysis

Data are reported as medians (interquartile ranges [IQRs]) or counts (percentages), depending on the type of variables. Continuous and categorical variables were compared using Student's *t*-test or the chi-squared test. Liver stiffness and steatosis across fibrosis and steatosis stages were compared using the Kruskal–Wallis test, with Dunn's multiple comparisons test for pairwise comparisons. Discriminatory performance of MRE and MRI-PDFF was assessed using areas under the receiver operating characteristic curves (AUCs) and corresponding 95% confidence intervals (CIs) were calculated. Optimal cut-off values were determined at the highest Youden index. Sensitivity, specificity, positive predictive value, and negative predictive value were calculated at each threshold. Spearman correlation coefficients (*r*) and their corresponding *p*-values were used to evaluate correlations between liver stiffness and clinical variables. Variables with a $p < 0.1$ in univariable Cox regression were included in multivariable Cox regression models to identify independent predictors of 1-year graft loss after LT. Statistical analyses were performed using R software (version 4.3.2; R Foundation for Statistical Computing, Vienna, Austria) and GraphPad Prism (version 10.4.1; GraphPad Software Inc., San Diego, CA). Statistical significance was set at $p < 0.05$.

3 | Results

3.1 | Baseline Characteristics

The baseline characteristics of the study population are summarized in Table 1. The median recipient age was 57.0 years, and 135 (72.2%) were male. The median body mass index (BMI) of the recipients was 24.5 kg/m^2. The most prevalent underlying liver disease was hepatitis B virus infection ($n = 103$, 55.1%), followed by alcoholic liver disease ($n = 40$, 21.4%) and hepatitis C virus infection ($n = 14$, 7.5%). HCC was present in 133 (71.1%) patients. A total of 118 (63.1%) patients were classified as having CTP Class A liver function, 49 (26.2%) as Class B, and 20 (10.7%) as Slass C. The median MELD score was 11.0.

The median donor age was 33.0 years, with a BMI of 23.1 kg/m^2. The median graft-to-recipient weight ratio was 1.1, and the median graft macrovesicular steatosis was 5.0%. The median operative time was 545 min. The median hospital stay was 22.0 days. The median liver stiffness by MRE and fat fraction by MRI-PDFF were 6.5 kPa and 2.3%, respectively.

3.2 | Distribution of Liver Histology

Fibrosis Stages 2, 3, 4a, 4b, and 4c were identified in 3 (1.6%), 19 (10.2%), 10 (5.3%), 48 (25.7%), and 107 (57.0%) patients, respectively (Figure S1). Steatosis Grades 0, 1, and 2 were identified in 111 (59.4%), 73 (39.0%), and 3 (1.6%) patients, respectively. The majority of patients ($n = 147$, 78.6%) exhibited moderate (A2) inflammatory activity.

3.3 | Liver Stiffness by MRE According to Fibrosis Stage

Median liver stiffness values by MRE corresponding to fibrosis Stages 2, 3, 4a, 4b, and 4c were 2.96 (IQR: 2.52–4.20), 3.80 (IQR: 3.29–4.30), 4.26 (IQR: 3.47–4.94), 5.33 (IQR: 4.37–6.39), and 8.18 (IQR: 6.53–10.58) kPa, respectively. Liver stiffness by MRE significantly differed across fibrosis Stages 2, 3, and 4 (Figure 1A), as well as when Stage 4 was further subclassified into Stages 4a, 4b, and 4c (Figure 1B) (both Kruskal–Wallis $p < 0.001$). Pairwise comparisons showed no significant difference between Stages 2 and 3 ($p > 0.05$). Significant differences were observed between Stages 4a and 4c ($p < 0.0001$) and between Stages 4b and 4c ($p < 0.0001$). However, no significant differences were observed between Stages 3 and 4a nor between Stages 4a and 4b (all $p > 0.05$), despite a stepwise increase in liver stiffness values across these stages (Figure 1B).

3.4 | Fat Fraction by MRI-PDFF According to Steatosis Grade

The median fat fractions by MRI-PDFF corresponding to steatosis Grades 0, 1, and 2 were 2.14% (IQR: 1.69–2.43), 3.47% (IQR: 2.45–5.24), and 9.76% (IQR: 4.22–18.62), respectively. The fat fraction measured by MRI-PDFF significantly differed according to steatosis grade (Kruskal–Wallis $p < 0.001$) (Figure 2). While significant differences were observed between Grades 0 and 1 ($p < 0.001$), as well as between Grades 0 and 2 ($p = 0.002$), no significant difference was observed between Grades 1 and 2 ($p = 0.406$).

3.5 | AUC of MRE and MRI-PDFF in Staging Fibrosis and Steatosis

The AUCs of MRE and MRI-PDFF in staging fibrosis and steatosis are summarized in Table 2. The diagnostic accuracy of

TABLE 1 | Baseline characteristics ($N = 187$).

Characteristic	Value	Characteristic	Value
Age	57.0 [52.0;62.0]	Donor age	33.0 [26.0;44.0]
Male sex	135 (72.2)	Male donor	102 (54.5)
Weight, kg	68.2 ± 11.1	Donor BMI, kg/m^2	23.1 [21.2;25.2]
Height, cm	166.7 ± 8.2	Macrovesicular steatosis of graft, %	5.0 [0.0;5.0]
BMI, kg/m^2	24.5 ± 3.4	GRWR	1.1 [0.9;1.2]
Dyslipidemia	46 (24.6)	Operation time, min	545.0 [484.5;610.5]
Hypertension	59 (31.6)	Warm ischemic time, min	42.0 [34.5;53.0]
Diabetes mellitus	68 (36.4)	Cold ischemic time, min	120.0 [96.0; 144.0]
Cardiovascular disease	15 (8.0)	RBC transfusion, packs	2.0 [0.0;6.0]
Underlying liver disease		Intraoperative CRRT	2 (1.1)
HBV	103 (55.1)	Simultaneous splenectomy	18 (9.6)
HCV	14 (7.5)	Hospital stay, days	22.0 [17.0;33.0]
Alcoholic	40 (21.4)	Postoperative ICU stay, days	4.0 [3.0;4.0]
Autoimmune	7 (3.7)	Laboratory profile	
Others	23 (12.3)	Platelet count, 10^3/uL	77.0 [58.0;115.0]
HCC	133 (71.1)	Total bilirubin, mg/dL	1.4 [0.9;2.0]
Clinical cirrhosis[a]	181 (96.8)	Alkaline phosphatase, IU/L	88.0 [68.0;123.0]
Ascites		AST, IU/L	34.0 [25.5;47.0]
No/minimal	119 (63.6)	ALT, IU/L	18.0 [13.0;25.0]
Moderate	46 (24.6)	Serum albumin, g/dL	3.4 ± 0.6
Large/refractory	22 (11.8)	Fasting glucose, mg/dL	107.0 [90.0;141.0]
Esophageal varix		GGT, IU/L	41.5 [25.0;81.0]
No	109 (58.3)	Total cholesterol, mg/dL	122.0 [98.0;146.0]
Varix without bleeding	19 (10.2)	HDL-cholesterol, mg/dL	36.0 [28.0;45.0]
Varix with bleeding	59 (31.6)	Triglycerides, mg/dL	69.0 [51.0;101.0]
Encephalopathy		INR	1.2 [1.1;1.3]
No	174 (93.0)	AFP, ng/mL	5.0 [2.7; 11.1]
Mild	12 (7.0)	DCP, mAU/mL	47.5 [27.0;136.0]
Child–Pugh (A/B/C)	118 (63.1) /49 (26.2) /20 (10.7)	C-reactive protein, mg/L	2.2 [0.8;6.4]
Pretransplant MELD	11.0 [9.0;15.0]	Liver stiffness by MRE, kPa	6.5 [4.5;9.0]
ABO incompatibility	58 (31.0)	MRI-PDFF, %	2.3 [1.9;3.4]
Living donor	185 (98.9)		

Note: Data are presented as *n* (%) or median [interquartile range], unless otherwise indicated.
[a]Clinical cirrhosis was defined based on a combination of radiologic findings suggestive of cirrhosis, clinical manifestations of portal hypertension, and thrombocytopenia (platelet count < 150000/μL).
Abbreviations: AFP, alpha-fetoprotein; ALT, alanine aminotransferase; AST, aspartate aminotransferase; BMI, body mass index; CRRT; continuous renal replacement therapy; DCP, des-gamma carboxyprothrombin; GGT, gamma-glutamyl transferase; GRWR, graft-to-recipient weight ratio; HCC, hepatocellular carcinoma; HDL, high density lipoprotein; ICU, intensive care unit; INR, international normalized ratio; MELD, model for end-stage liver disease; MRE, magnetic resonance elastography, MRI-PDFF, magnetic resonance imaging-based proton density fat fraction; RBC, red blood cell.

MRE for liver fibrosis staging showed an AUC of 0.92 (95% CI: 0.87–0.97) for differentiating Stages 2 and 3 vs. Stage 4 fibrosis, with a sensitivity of 79.4% and a specificity of 95.5% at a threshold of 4.76 kPa. The performance remained robust in distinguishing different fibrosis stages, with AUC values of 0.91 (95% CI: 0.86–0.96) (Stages 2–4a vs. Stage 4b,c) and 0.85 (95% CI: 0.79–0.91) (Stages 2–4b vs. Stage 4c), with respective threshold values of 5.02 and 6.43 kPa.

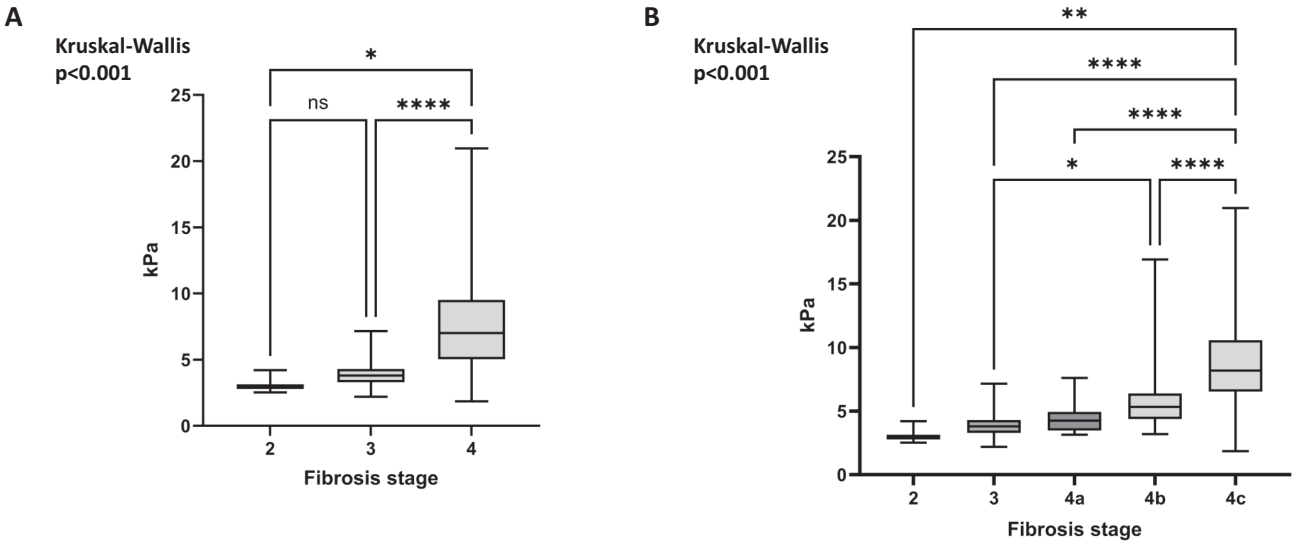

FIGURE 1 | Liver stiffness measured by MRE according to fibrosis stages F2, F3, and F4 (A) and subclassification of Stage 4 fibrosis into Laennec Stages 4a, 4b, and 4c (B), demonstrating a progressive increase in liver stiffness with histologic severity. Statistical analysis was performed using the Kruskal–Wallis test followed by Dunn's post hoc test. ns, nonspecific; *$p < 0.05$, **$p < 0.01$, ***$p < 0.001$, ****$p < 0.0001$.

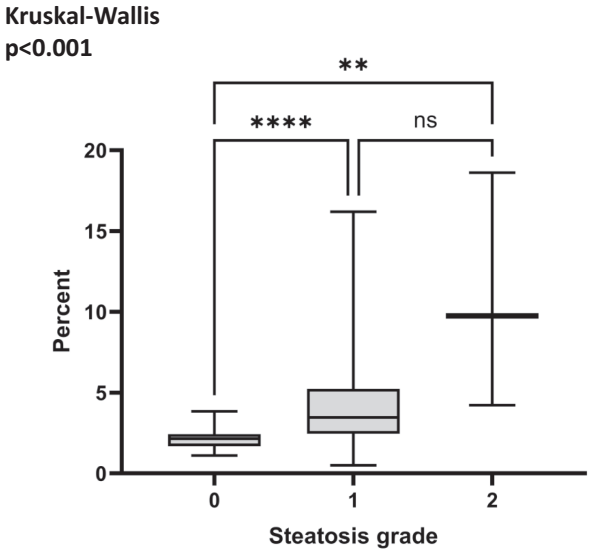

FIGURE 2 | Fat fraction measured by MRI-PDFF according to histologic steatosis grade. Statistical analysis was performed using the Kruskal–Wallis test followed by Dunn's post hoc test. ns, nonspecific; *$p < 0.05$, **$p < 0.01$, ***$p < 0.001$, ****$p < 0.0001$.

For MRI-PDFF in assessing hepatic steatosis, the AUC for distinguishing Grade 0 from Grades 1 to 2 steatosis was 0.83 (95% CI: 0.76–0.89), with a sensitivity of 68.4% and specificity of 89.2% at a threshold of 2.80%. When differentiating Grades 0–1 from Grade 2, MRI-PDFF demonstrated high diagnostic accuracy, with an AUC of 0.95 (95% CI: 0.87–1.00), sensitivity of 100%, and specificity of 86.4% at a threshold of 4.19%.

Receiver operating characteristic curves for MRE and MRI-PDFF for diagnosing fibrosis stage and steatosis grade are depicted in Figure S2.

3.6 | Comparisons of Patients With and Without Cirrhosis or Severe Cirrhosis

Based on the threshold values of liver stiffness by MRE from AUC analyses, patients were classified into noncirrhosis (< 4.76 kPa, $n = 55$ [29.4%]) and cirrhosis (≥ 4.76 kPa, $n = 132$ [70.6%]) groups or nonsevere cirrhosis (< 6.43 kPa, $n = 92$ [48.1%]) and severe cirrhosis (≥ 6.43 kPa, $n = 95$ [50.8%]) groups.

Comparisons between patients with and without cirrhosis or severe cirrhosis are summarized in Table 3. Patients with cirrhosis or severe cirrhosis had significantly higher MELD scores (12.0 vs. 11.0, $p = 0.006$; 13.0 vs. 11.0, $p < 0.001$) and were more likely to present with moderate-to-large/refractory ascites ($p = 0.007$, $p = 0.002$) and esophageal varices ($p = 0.03$, $p = 0.012$). Severe cirrhosis was further associated with a history of encephalopathy ($p = 0.025$). CTP Class B or C was more frequently observed in patients with cirrhosis (41.6% vs. 25.4%, $p = 0.055$) and was significantly more prevalent in those with severe cirrhosis (50.5% vs. 22.9%, $p < 0.001$).

In terms of laboratory findings, patients with cirrhosis and severe cirrhosis had lower platelet counts ($p = 0.027$, $p = 0.030$) and serum albumin levels (both $p < 0.001$) and higher levels of total bilirubin ($p = 0.005$, $p < 0.001$), alkaline phosphatase ($p = 0.011$, $p = 0.002$), AST ($p = 0.008$, $p < 0.001$), INR (both $p < 0.001$), and C-reactive protein ($p = 0.006$, $p = 0.026$). From a surgical perspective, patients with cirrhosis or severe cirrhosis required more intraoperative red blood cell (RBC) transfusions (3.0 vs. 0.0 packs, both $p < 0.001$).

3.7 | Association Between Liver Stiffness by MRE and Clinical Variables

Correlation analysis of liver stiffness by MRE with clinical and laboratory parameters that differed significantly between

TABLE 2 | AUC of MRE and MRI-PDFF for diagnosis of fibrosis and steatosis.

	AUC (95% CI)	Threshold, kPa	Sensitivity, %	Specificity, %	PPV, %	NPV, %
MRE						
Stages 2 and 3 ($n=22$) vs. Stage 4 ($n=165$)	0.92 (0.87–0.97)	4.76	79.4	95.5	99.2	38.3
Stages 2–4a ($n=32$) vs. Stages 4b and 4c ($n=155$)	0.91 (0.86–0.96)	5.02	80.0	93.8	98.4	49.2
Stages 2–4b ($n=80$) vs. Stage 4c ($n=107$)	0.85 (0.79–0.91)	6.43	77.6	85.0	87.4	74.0
	AUC (95% CI)	Threshold, %	Sensitivity, %	Specificity, %	PPV, %	NPV, %
MRI-PDFF						
Grade 0 ($n=111$) vs. Grades 1 and 2 ($n=76$)	0.83 (0.76–0.89)	2.80	68.4	89.2	81.2	80.5
Grades 0 and 1 ($n=184$) vs. Grade 2 ($n=3$)	0.95 (0.87–1.00)	4.19	100.0	86.4	10.7	100.0

Abbreviations: AUC, area under the receiver operator characteristic curve; CI, confidence interval; MRE, magnetic resonance elastography, MRI-PDFF, magnetic resonance imaging-based proton density fat fraction; NPV, negative predictive value; PPV, positive predictive value.

cirrhosis and noncirrhosis or between severe cirrhosis and non-severe cirrhosis groups showed a positive correlation with the MELD score ($r=0.2317$, $p=0.001$), RBC transfusion volume ($r=0.4334$, $p<0.001$), total bilirubin ($r=0.3034$, $p<0.001$), alkaline phosphatase ($r=0.2669$, $p<0.001$), AST ($r=0.2791$, $p<0.001$), and INR ($r=0.4336$, $p<0.001$) (Figure 3). A negative correlation was observed with platelet count ($r=-0.1554$, $p=0.033$) and serum albumin ($r=-0.4026$, $p<0.001$).

3.8 | Independent Risk Factors for 1-Year Graft Loss After LT

During a median follow-up of 29.2 months (IQR: 15.2–43.8) after LT, graft loss occurred in 27 cases (7 graft failures leading to re-transplantation and 20 patient deaths) within 1-year post-LT. A higher MELD score (hazard ratio [HR], 1.07; 95% CI, 1.02–1.11), longer operative time (HR, 1.00; 95% CI, 1.00–1.01), and greater RBC transfusion volume (HR, 1.09; 95% CI, 1.01–1.17) were significantly associated with an increased risk of 1-year graft loss (Table S1). MRE-defined thresholds for cirrhosis (≥4.76 kPa) and severe cirrhosis (≥6.43 kPa) were not significantly associated with 1-year graft loss ($p=0.579$ and $p=0.978$, respectively, in univariate analyses).

4 | Discussion

Using comprehensive histologic evaluation of explant livers at LT, this retrospective cohort study demonstrated high diagnostic accuracy of MRE and MRI-PDFF for detecting cirrhosis and hepatic steatosis, respectively. Although the diagnostic performance of MRE and MRI-PDFF has been well-established in previous studies, our study provides additional insights by evaluating their performance specifically in a cirrhosis-enriched LT population and by correlating imaging findings with detailed histologic and clinical parameters. To our knowledge, this is the first study to evaluate the diagnostic performance of MRE for substaging cirrhosis according to histologic fibrosis burden, supported by comprehensive assessment of the entire explanted liver. Notably, an MRE-derived threshold for severe cirrhosis (F4c) effectively distinguished patients based on MELD score and CTP classifications, history of decompensation, and key laboratory parameters. Additionally, liver stiffness measured by MRE was significantly correlated with intraoperative RBC transfusion volume, which was independently associated with 1-year graft loss. Importantly, the consistency of MRE and MRI-PDFF diagnostic accuracy in our cohort with prior literature suggests that our study population was not substantially skewed, thereby reinforcing the reliability of subsequent outcome analyses. These findings support the utility of MRI-based diagnostics in advanced fibrosis and suggest that MRE may aid in the noninvasive risk stratification and monitoring of patients with cirrhosis.

This study has several unique clinical implications. First, prior studies showed high diagnostic accuracy of MRE for detecting cirrhosis in single-etiology cohorts, such as patients with MASLD (AUCs 0.87–0.97) [11, 19–22] or chronic hepatitis B (CHB) (AUCs 0.894–0.987) [23–26]. Despite the predominance of CHB and alcohol-related disease, this study adds value by demonstrating the utility of MRE in a more diverse CLD cohort. This study established a diagnostic cut-off for cirrhosis of 4.76 kPa, which is higher than the previously reported values in CHB (3.46–4.33 kPa) [23–26]. Using this threshold, 90.0% of patients with alcoholic liver disease, compared with 58.3% of those with CHB, were classified as cirrhotic, suggesting the alcoholic subgroup (21.4% of cohort) may have contributed to the elevated threshold.

Second, this study demonstrated the high diagnostic performance of MRE in identifying Laennec Stages F4b and F4c. In a previous study utilizing the Laennec system [14], patients with F4b and 4c had significantly higher risks of hepatic

TABLE 3 | Characteristics between patients with or without cirrhosis and severe cirrhosis.

Characteristic	Noncirrhosis (<4.76 kPa) (*n* = 55)	Cirrhosis (≥4.76 kPa) (*n* = 132)	*p*	Nonsevere cirrhosis (<6.43 kPa) (*n* = 92)	Severe cirrhosis (≥6.43 kPa) (*n* = 95)	*p*
Age	56.0 [51.5;62.0]	57.0 [52.0;61.5]	0.674	57.0 [52.0;62.0]	57.0 [52.0;61.0]	0.818
Male sex	44 (80.0)	91 (68.9)	0.174	72 (78.3)	63 (66.3)	0.097
BMI, kg/m^2	24.3 ± 2.7	24.6 ± 3.6	0.56	24.1 ± 2.9	24.9 ± 3.7	0.108
Dyslipidemia	16 (29.1)	30 (22.7)	0.463	26 (28.3)	20 (21.1)	0.33
Hypertension	17 (30.9)	42 (31.8)	1.000	26 (28.3)	33 (34.7)	0.426
Diabetes mellitus	20 (36.4)	48 (36.4)	1.000	32 (34.8)	36 (37.9)	0.772
Cardiovascular disease	4 (7.3)	11 (8.3)	1.000	4 (4.3)	11 (11.6)	0.121
Underlying liver disease			0.001			< 0.001
HBV	43 (78.2)	60 (45.5)		65 (70.7)	38 (40.0)	
HCV	2 (3.6)	12 (9.1)		5 (5.4)	9 (9.5)	
Alcoholic	4 (7.3)	36 (27.3)		10 (10.9)	30 (31.6)	
Autoimmune	3 (5.5)	4 (3.0)		4 (4.3)	3 (3.2)	
Others	3 (5.5)	20 (15.2)		8 (8.7)	15 (15.8)	
HCC	44 (80.0)	89 (67.4)	0.121	72 (78.3)	61 (64.2)	0.05
Ascites			0.007			0.002
No/minimal	44 (80.0)	75 (56.8)		70 (76.1)	49 (51.6)	
Moderate	9 (16.4)	37 (28.0)		16 (17.4)	30 (31.6)	
Large/refractory	2 (3.6)	20 (15.2)		6 (6.5)	16 (16.8)	
Esophageal varix			0.03			0.012
No	38 (69.1)	71 (53.8)		63 (68.5)	46 (48.4)	
Varix without bleeding	16 (29.1)	43 (32.6)		24 (26.1)	35 (36.8)	
Varix with bleeding	1 (1.8)	18 (13.6)		5 (5.4)	14 (14.7)	
Encephalopathy			0.143			0.025
No	54 (98.2)	120 (90.9)		90 (97.8)	84 (88.4)	
Mild	1 (1.8)	12 (9.1)		2 (2.2)	11 (11.6)	
Child–Pugh (A/B/C)	41 (74.5) /12 (21.8) /2 (3.6)	77 (58.3) /37 (28.0) /18 (13.6)	0.055	71 (77.2) /19 (20.7) /2 (2.2)	47 (49.5) /30 (31.6) /18 (18.9)	< 0.001

(Continues)

TABLE 3 | (Continued)

Characteristic	Noncirrhosis (<4.76 kPa) (*n* = 55)	Cirrhosis (≥4.76 kPa) (*n* = 132)	*p*	Nonsevere cirrhosis (<6.43 kPa) (*n* = 92)	Severe cirrhosis (≥6.43 kPa) (*n* = 95)	*p*
Pretransplant MELD	11.0 [7.0;13.0]	12.0 [9.0;16.0]	0.006	11.0 [7.0;13.0]	13.0 [9.0;17.0]	< 0.001
ABO incompatibility	10 (18.2)	48 (36.4)	0.023	27 (29.3)	31 (32.6)	0.744
Living donor	55 (100.0)	130 (98.5)	0.891	92 (100.0)	93 (97.9)	0.491
Donor age	33.0 [25.0;43.0]	33.0 [26.0;45.0]	0.675	33.0 [25.0;42.5]	34.0 [26.0;45.5]	0.587
Male donor	23 (41.8)	79 (59.8)	0.036	48 (52.2)	54 (56.8)	0.621
Donor BMI	22.7 [21.2;24.4]	23.4 [21.1;25.7]	0.182	22.7 [21.2;24.8]	23.3 [21.1;25.9]	0.266
Macrovesicular steatosis of graft, %	2.0 [0.0; 5.0]	5.0 [0.0; 5.0]	0.136	5.0 [0.0; 5.0]	5.0 [0.0; 5.0]	0.942
GRWR	1.1 [0.9; 1.2]	1.1 [0.9; 1.2]	0.760	1.1 [0.9; 1.2]	1.1 [0.9; 1.2]	0.705
Operation time, min	546.0 [486.0;646.5]	544.9 [481.5;600.0]	0.610	542.5 [486.0;609.9]	546.0 [477.0;610.5]	0.899
Warm ischemic time, min	44.0 [34.5;51.5]	41.0 [34.5;55.0]	0.522	43.0 [34.0;54.5]	41.0 [35.0;51.5]	0.428
Cold ischemic time, min	120.0 [103.5;144.0]	120.0 [96.0;139.5]	0.340	120.0 [102.0;142.0]	120.0 [96.0;144.0]	0.703
RBC transfusion, packs	0.0 [0.0; 3.0]	3.0 [1.0; 7.0]	< 0.001	0.0 [0.0; 3.0]	3.0 [2.0; 8.0]	< 0.001
Intraoperative CRRT	0 (0.0)	2 (1.5)	0.891	0 (0.0)	2 (2.1)	0.491
Simultaneous splenectomy	7 (12.7)	11 (8.3)	0.512	9 (9.8)	9 (9.5)	1.000
Hospital stay, days	22.0 [16.0;30.0]	23.0 [18.0;33.0]	0.258	22.0 [16.0;32.0]	23.0 [18.5;33.0]	0.307
Postoperative ICU stay, days	4.0 [3.0; 4.0]	3.0 [3.0; 4.0]	0.037	4.0 [3.0; 4.0]	3.0 [3.0; 4.0]	0.344
Laboratory profile						
Platelet count, 10^3/uL	105.0 [59.5;144.0]	73.0 [58.0;99.0]	0.027	89.0 [59.5;134.5]	67.0 [57.0;95.0]	0.030
Total bilirubin, mg/dL	1.1 [0.7; 1.9]	1.5 [1.0; 2.2]	0.005	1.1 [0.7; 1.9]	1.5 [1.1; 2.8]	< 0.001
Alkaline phosphatase, IU/L	73.0 [61.5;109.5]	94.5 [72.5;129.0]	0.011	83.0 [67.0;113.0]	105.0 [74.5;134.5]	0.002
AST, IU/L	29.0 [23.0;39.0]	36.0 [27.0;51.0]	0.008	30.0 [25.0;40.0]	39.0 [28.5;57.0]	< 0.001
ALT, IU/L	18.0 [14.0;26.5]	18.5 [13.0;24.0]	0.418	20.0 [17.0;24.0]	17.0 [12.0;24.0]	0.061
Serum albumin, g/dL	3.6 ± 0.7	3.2 ± 0.5	< 0.001	3.6 ± 0.4	3.1 ± 0.5	< 0.001
Fasting glucose, mg/dL	100.0 [88.0;144.5]	110.0 [90.0;140.5]	0.33	110.0 [87.0;146.0]	109.0 [90.0;139.5]	0.752
GGT, IU/L	34.0 [23.0;55.5]	50.0 [27.5;84.0]	0.027	50.0 [25.0;106.0]	48.5 [28.0;80.0]	0.196

(Continues)

TABLE 3 | (Continued)

Characteristic	Noncirrhosis (< 4.76 kPa) (*n* = 55)	Cirrhosis (≥ 4.76 kPa) (*n* = 132)	*p*	Nonsevere cirrhosis (< 6.43 kPa) (*n* = 92)	Severe cirrhosis (≥ 6.43 kPa) (*n* = 95)	*p*
Total cholesterol, mg/dL	123.0 [93.5;144.0]	121.0 [99.0;149.0]	0.961	130.0 [115.5;156.5]	116.0 [97.0;145.5]	0.12
HDL-cholesterol, mg/dL	35.0 [30.0;44.0]	36.0 [27.0;46.0]	0.749	40.0 [28.5;46.0]	35.0 [26.0;45.0]	0.374
Triglycerides, mg/dL	70.0 [51.0;101.0]	69.0 [51.0;101.0]	0.91	87.5 [61.0;107.5]	62.0 [51.0;85.0]	0.154
INR	1.1 [1.0; 1.2]	1.2 [1.1; 1.4]	< 0.001	1.1 [1.0; 1.2]	1.2 [1.1; 1.4]	< 0.001
AFP, ng/mL	4.7 [2.1;11.1]	5.0 [3.0;12.0]	0.279	4.5 [3.0;12.8]	5.1 [3.0;12.0]	0.345
DCP, mAU/mL	39.0 [27.0;95.0]	52.0 [26.5;209.0]	0.148	40.0 [24.0;224.0]	56.0 [29.0;193.5]	0.134
C-reactive protein, mg/L	1.4 [0.5; 4.9]	2.7 [1.1; 6.8]	0.006	2.4 [1.0; 6.4]	2.9 [1.1; 6.9]	0.026

Note: Data are *n* (%) or median [interquartile range], unless otherwise indicated.
Abbreviations: AFP, alpha-fetoprotein; ALT, alanine aminotransferase; AST, aspartate aminotransferase; BMI, body mass index; CRRT; continuous renal replacement therapy; DCP, des-gamma carboxyprothrombin; GGT, gamma-glutamyl transferase; GRWR, graft-to-recipient weight ratio; HCC, hepatocellular carcinoma; HDL, high density lipoprotein; ICU, intensive care unit; INR, international normalized ratio; MELD, model for end-stage liver disease; RBC, red blood cell.

decompensation, HCC, and liver-related death, compared with those with Stage 3. Stage 4a showed only a trend toward increased risk relative to Stage 3. These findings suggest that clinically relevant transitions in advanced fibrosis may occur between Stages 3 and 4a and 4b and 4c. Consistent with this, liver stiffness measurements by MRE in this study were significantly higher in Stages 4b and 4c than in Stage 3, with no difference between Stages 3 and 4a. Thus, the MRE-derived cut-offs for Stages 4b and 4c (5.02 kPa) and Stage 4c (6.43 kPa) may represent meaningful thresholds in the progression of advanced fibrosis, offering additional prognostic insight beyond conventional cut-offs for Stage 4.

Third, although liver stiffness by MRE was not an independent risk factor for 1-year graft survival, it showed significant correlations with mortality-related factors, such as MELD score and RBC transfusion volume during LT [27–29]. Several studies have reported that intraoperative transfusion requirements are difficult to predict based on preoperative variables [29–31]. Given that transfusion needs during LT typically reflect the severity of portal hypertension and coagulopathy [32, 33], MRE appeared to effectively capture this physiological burden. The observed correlation between liver stiffness by MRE and intraoperative RBC transfusion volume suggests that preoperative MRE may provide useful descriptive information regarding the intraoperative course.

Fourth, while MRI-PDFF demonstrated an AUC of 0.83 for detecting hepatic steatosis, its diagnostic performance—particularly the cut-off value of 2.80%—was lower than previously reported. A recent meta-analysis proposed a cut-off of 5.7% for diagnosing steatosis in MASLD cohorts, with an AUC of 0.97 [34]. This discrepancy may reflect differences in study populations. Unlike MASLD-focused studies, our cohort included diverse etiologies, with over half of cases showing no hepatic steatosis and a median fat fraction for Grade 1 as low as 3.47%. Even when compared with a recent study of healthy liver donor candidates—reporting a 3.5% cut-off with an AUC of 0.920 [35]—our threshold and accuracy remained lower. Two factors may explain this. First, MRI-PDFF values are reported to be underestimated in advanced fibrosis because of increased tissue water and iron, which reduce fat signals in MRI [36, 37], potentially contributing to the lower values in our cohort with a high prevalence of cirrhosis. Next, in this study, MRI-PDFF was calculated as the mean across four ROIs, whereas the histologic grading reflected the highest grade among seven samples. This may result in a lower cut-off than biopsy-based studies. Given the small number of patients with moderate-to-severe steatosis in this study, the potential attenuation of MRI-PDFF performance and the relatively low cut-off observed in cirrhotic populations warrant validation in external cohorts with adequate representation across steatosis grades.

This study is strengthened by the inclusion of a large number of patients with cirrhosis and the use of robust histologic evaluation of explant livers, minimizing discrepancies commonly associated with liver biopsy [38]. Nevertheless, several limitations should be acknowledged. First, owing to its retrospective design and including only patients who underwent pretransplant MRI, our cohort was enriched for elective, lower MELD recipients, with a predominance of living donor transplantation and a

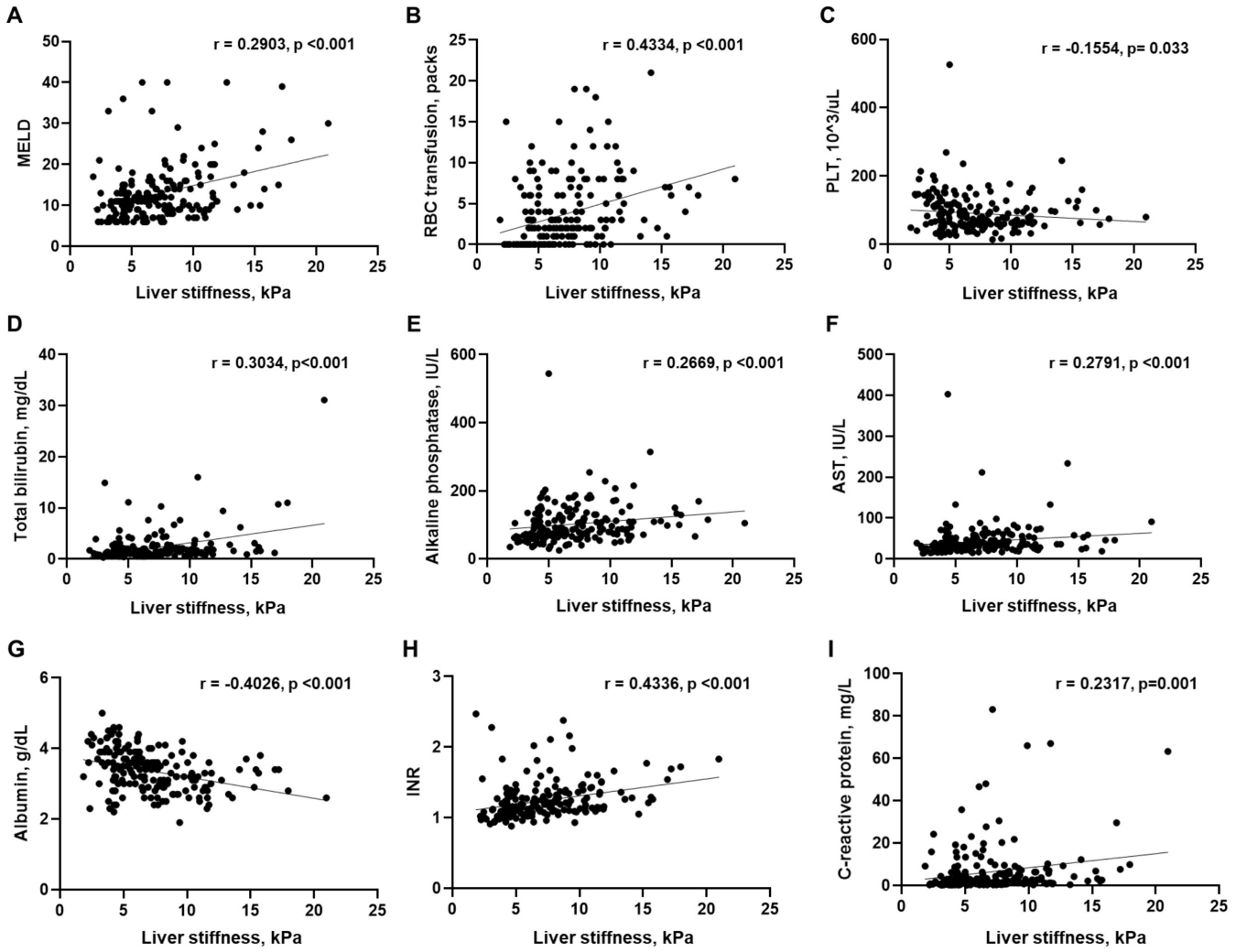

FIGURE 3 | Correlation between liver stiffness measured by MRE and clinical variables. Correlation coefficients (*r*) and *p*-values were calculated using Spearman's correlation analysis. AST, aspartate aminotransferase; INR, international normalized ratio; MELD, model for end-stage liver disease; PLT, platelet; RBC, red blood cell.

relatively high proportion of patients with HCC, which introduces inevitable selection bias. Therefore, the proposed cut-off values may not be applicable to urgent or high-acuity transplant candidates nor to nontransplant cirrhosis populations. Second, since CHB infection and alcoholic cirrhosis are the most common underlying liver diseases leading to LT in South Korea, the MRI-based cut-off values for cirrhosis, severe cirrhosis, and hepatic steatosis may limit generalizability. Third, despite including a high proportion of HCC patients in this cohort, the scope of this study did not include exploring the potential relationship between MRE/MRI-PDFF values and posttransplant HCC recurrence rate, due to the relatively short follow-up time and limited number of patients. Fourth, although vibration-controlled transient elastography is a widely used noninvasive test for liver fibrosis, only 21 patients (11.2%) in our study cohort underwent this exam, which limited our ability to compare its diagnostic performance with MRE and MRI-PDFF. Finally, liver stiffness by MRE and fat fraction by MRI-PDFF were manually measured rather than automatically derived, introducing potential intra-observer variability despite being assessed by a single radiologist.

In conclusion, MRE and MRI-PDFF demonstrated excellent to good diagnostic accuracy in detecting cirrhosis and hepatic steatosis, respectively, in patients undergoing LT. MRE further subclassified cirrhosis, correlating with liver function, decompensation history, and transfusion requirements. These findings suggest the clinical utility of MRI-based diagnostics in CLD, with MRE serving as a valuable noninvasive tool for assessing cirrhosis severity.

Acknowledgments

The authors have nothing to report.

Funding

The authors have nothing to report.

Data Availability Statement

The datasets generated and/or analyzed during this study are available on reasonable request.

References

1. M. Ekstedt, H. Hagström, P. Nasr, et al., "Fibrosis Stage Is the Strongest Predictor for Disease-Specific Mortality in NAFLD After up to 33 Years of Follow-Up," *Hepatology* 61 (2015): 1547–1554.

2. C. Lackner, R. E. Stauber, S. Davies, et al., "Development and Prognostic Relevance of a Histologic Grading and Staging System for Alcohol-Related Liver Disease," *Journal of Hepatology* 75 (2021): 810–819.

3. G. Cholankeril, J. R. Kramer, J. Chu, et al., "Longitudinal Changes in Fibrosis Markers Are Associated With Risk of Cirrhosis and Hepatocellular Carcinoma in Non-Alcoholic Fatty Liver Disease," *Journal of Hepatology* 78 (2023): 493–500.

4. I. L. Nalbantoglu and E. M. Brunt, "Role of Liver Biopsy in Nonalcoholic Fatty Liver Disease," *World Journal of Gastroenterology* 20 (2014): 9026–9037.

5. M. N. Kim, J. W. Han, J. An, et al., "KASL Clinical Practice Guidelines for Noninvasive Tests to Assess Liver Fibrosis in Chronic Liver Disease," *Clinical and Molecular Hepatology* 30 (2024): S5–s105.

6. A. Berzigotti, E. Tsochatzis, J. Boursier, et al., "EASL Clinical Practice Guidelines on Non-Invasive Tests for Evaluation of Liver Disease Severity and Prognosis - 2021 Update," *Journal of Hepatology* 75 (2021): 659–689.

7. Y. N. Zhang, K. J. Fowler, A. Ozturk, et al., "Liver Fibrosis Imaging: A Clinical Review of Ultrasound and Magnetic Resonance Elastography," *Journal of Magnetic Resonance Imaging* 51 (2020): 25–42.

8. Y. E. Chon, Y. J. Jin, J. An, et al., "Optimal Cut-Offs of Vibration-Controlled Transient Elastography and Magnetic Resonance Elastography in Diagnosing Advanced Liver Fibrosis in Patients With Nonalcoholic Fatty Liver Disease: A Systematic Review and Meta-Analysis," *Clinical and Molecular Hepatology* 30 (2024): S117–s33.

9. H. Xiao, M. Shi, Y. Xie, and X. Chi, "Comparison of Diagnostic Accuracy of Magnetic Resonance Elastography and Fibroscan for Detecting Liver Fibrosis in Chronic Hepatitis B Patients: A Systematic Review and Meta-Analysis," *PLoS ONE* 12 (2017): e0186660.

10. Q. Gu, L. Cen, J. Lai, et al., "A Meta-Analysis on the Diagnostic Performance of Magnetic Resonance Imaging and Transient Elastography in Nonalcoholic Fatty Liver Disease," *European Journal of Clinical Investigation* 51 (2021): e13446.

11. A. Nogami, M. Yoneda, M. Iwaki, et al., "Diagnostic Comparison of Vibration-Controlled Transient Elastography and MRI Techniques in Overweight and Obese Patients With NAFLD," *Scientific Reports* 12 (2022): 21925.

12. S. Sharma, K. Khalili, and G. C. Nguyen, "Non-Invasive Diagnosis of Advanced Fibrosis and Cirrhosis," *World Journal of Gastroenterology* 20 (2014): 16820–16830.

13. M. Y. Kim, M. Y. Cho, S. K. Baik, et al., "Histological Subclassification of Cirrhosis Using the Laennec Fibrosis Scoring System Correlates With Clinical Stage and Grade of Portal Hypertension," *Journal of Hepatology* 55 (2011): 1004–1009.

14. S. U. Kim, H. J. Oh, I. R. Wanless, S. Lee, K. H. Han, and Y. N. Park, "The Laennec Staging System for Histological Sub-Classification of Cirrhosis Is Useful for Stratification of Prognosis in Patients With Liver Cirrhosis," *Journal of Hepatology* 57 (2012): 556–563.

15. G. Kim, S. S. Lee, S. K. Baik, et al., "The Need for Histological Subclassification of Cirrhosis: A Systematic Review and Meta-Analysis," *Liver International* 36 (2016): 847–855.

16. A. Rastogi, R. Maiwall, C. Bihari, et al., "Cirrhosis Histology and Laennec Staging System Correlate With High Portal Pressure," *Histopathology* 62 (2013): 731–741.

17. K. M. Pepin, C. L. Welle, F. F. Guglielmo, J. R. Dillman, and S. K. Venkatesh, "Magnetic Resonance Elastography of the Liver: Everything You Need to Know to Get Started," *Abdominal Radiology (NY)*. 47 (2022): 94–114.

18. J. Starekova, D. Hernando, P. J. Pickhardt, and S. B. Reeder, "Quantification of Liver Fat Content With CT and MRI: State of the Art," *Radiology* 301 (2021): 250–262.

19. C. C. Park, P. Nguyen, C. Hernandez, et al., "Magnetic Resonance Elastography vs Transient Elastography in Detection of Fibrosis and Noninvasive Measurement of Steatosis in Patients With Biopsy-Proven Nonalcoholic Fatty Liver Disease," *Gastroenterology* 152 (2017): 598–607.e2.

20. K. Imajo, Y. Honda, T. Kobayashi, et al., "Direct Comparison of US and MR Elastography for Staging Liver Fibrosis in Patients With Nonalcoholic Fatty Liver Disease," *Clinical Gastroenterology and Hepatology* 20 (2022): 908–17.e11.

21. J. Cui, E. Heba, C. Hernandez, et al., "Magnetic Resonance Elastography Is Superior to Acoustic Radiation Force Impulse for the Diagnosis of Fibrosis in Patients With Biopsy-Proven Nonalcoholic Fatty Liver Disease: A Prospective Study," *Hepatology* 63 (2016): 453–461.

22. K. Imajo, T. Kessoku, Y. Honda, et al., "Magnetic Resonance Imaging More Accurately Classifies Steatosis and Fibrosis in Patients With Nonalcoholic Fatty Liver Disease Than Transient Elastography," *Gastroenterology* 150 (2016): 626–37.e7.

23. J. E. Lee, J. M. Lee, K. B. Lee, et al., "Noninvasive Assessment of Hepatic Fibrosis in Patients With Chronic Hepatitis B Viral Infection Using Magnetic Resonance Elastography," *Korean Journal of Radiology* 15 (2014): 210–217.

24. S. K. Venkatesh, G. Wang, S. G. Lim, and A. Wee, "Magnetic Resonance Elastography for the Detection and Staging of Liver Fibrosis in Chronic Hepatitis B," *European Radiology* 24 (2014): 70–78.

25. W. Chang, J. M. Lee, J. H. Yoon, et al., "Liver Fibrosis Staging With MR Elastography: Comparison of Diagnostic Performance Between Patients With Chronic Hepatitis B and Those With Other Etiologic Causes," *Radiology* 280 (2016): 88–97.

26. H. S. Park, W. H. Choe, H. S. Han, et al., "Assessing Significant Fibrosis Using Imaging-Based Elastography in Chronic Hepatitis B Patients: Pilot Study," *World Journal of Gastroenterology* 25 (2019): 3256–3267.

27. A. Rana, H. Petrowsky, J. C. Hong, et al., "Blood Transfusion Requirement During Liver Transplantation Is an Important Risk Factor for Mortality," *Journal of the American College of Surgeons* 216 (2013): 902–907.

28. M. T. de Boer, M. C. Christensen, M. Asmussen, et al., "The Impact of Intraoperative Transfusion of Platelets and Red Blood Cells on Survival After Liver Transplantation," *Anesthesia and Analgesia* 106 (2008): 32–44.

29. J. B. Cywinski, J. M. Alster, C. Miller, D. P. Vogt, and B. M. Parker, "Prediction of Intraoperative Transfusion Requirements During Orthotopic Liver Transplantation and the Influence on Postoperative Patient Survival," *Anesthesia & Analgesia*. 118 (2014): 428–437.

30. A. Steib, G. Freys, C. Lehmann, C. Meyer, and G. Mahoudeau, "Intraoperative Blood Losses and Transfusion Requirements During Adult Liver Transplantation Remain Difficult to Predict," *Canadian Journal of Anaesthesia* 48 (2001): 1075–1079.

31. C. K. Pandey, A. Singh, K. Kajal, et al., "Intraoperative Blood Loss in Orthotopic Liver Transplantation: The Predictive Factors," *World Journal of Gastrointestinal Surgery* 7 (2015): 86–93.

32. P. Feltracco, M. Brezzi, S. Barbieri, et al., "Blood Loss, Predictors of Bleeding, Transfusion Practice and Strategies of Blood Cell Salvaging During Liver Transplantation," *World Journal of Hepatology* 5 (2013): 1–15.

33. M. Giabicani, P. Joly, S. Sigaut, et al., "Predictive Role of Hepatic Venous Pressure Gradient in Bleeding Events Among Patients With

Cirrhosis Undergoing Orthotopic Liver Transplantation," *JHEP Reports* 6 (2024): 101051.

34. N. Azizi, H. Naghibi, M. Shakiba, et al., "Evaluation of MRI Proton Density Fat Fraction in Hepatic Steatosis: A Systematic Review and Meta-Analysis," *European Radiology* 35 (2025): 1794–1807.

35. S. Park, J. H. Kwon, S. Y. Kim, et al., "Cutoff Values for Diagnosing Hepatic Steatosis Using Contemporary MRI-Proton Density Fat Fraction Measuring Methods," *Korean Journal of Radiology* 23 (2022): 1260–1268.

36. S. McPherson, J. R. Jonsson, G. J. Cowin, et al., "Magnetic Resonance Imaging and Spectroscopy Accurately Estimate the Severity of Steatosis Provided the Stage of Fibrosis Is Considered," *Journal of Hepatology* 51 (2009): 389–397.

37. S. J. Bawden, C. Hoad, P. Kaye, et al., "Comparing Magnetic Resonance Liver Fat Fraction Measurements With Histology in Fibrosis: The Difference Between Proton Density Fat Fraction and Tissue Mass Fat Fraction," *Magma* 36 (2023): 553–563.

38. B. A. Davison, S. A. Harrison, G. Cotter, et al., "Suboptimal Reliability of Liver Biopsy Evaluation Has Implications for Randomized Clinical Trials," *Journal of Hepatology*. 73 (2020): 1322–1332.

Supporting Information

Additional supporting information can be found online in the Supporting Information section. **Figure S1:** Distribution of histologic grades of fibrosis, steatosis, and inflammation. **Figure S2:** Receiver operator characteristic curves for MRE and MRI-PDFF for the diagnosis of fibrosis stage and steatosis grade. **Table S1:** Univariable and multivariable Cox regression analysis of factors for 1-year graft loss.